Polysulfone-based anion exchange membranes demonstrate excellent chemical stability and performance for the all-vanadium redox flow battery

Electronic Supplementary Information

*Min-suk Jung, Javier Parrondo, Christopher G. Arges and Vijay Ramani**

Center for Electrochemical Science and Engineering, Department of Chemical and Biological Engineering, Illinois Institute of Technology, 10 W. 33rd St., Chicago, IL 60616
*Corresponding author's e-mail: ramani@iit.edu

Experimental Procedures

Synthesis of chloromethylated polysulfone (CMPSF) and PSF-TMA$^+$Cl$^-$. CMPSF was synthesized via the Friedel-Crafts reaction following the procedure described by Avram and coworkers.[1] Details describing the chloromethylation procedure and fabrication of PSF-TMA$^+$Cl$^-$ used in our lab is given in our previously published work.[2] Note: higher molecular weight PSF (~75,000), Acros Organics, was used rather than the lower molecular weight PSF (~35,000) documented in our previous work. [2]

The PSF-TMA$^+$ Cl$^-$ film was then ion-exchanged to sulfate form by immersing in 1 M Na_2SO_4 solution at room temperature during 24 hours. The 1 M Na_2SO_4 solution was changed several times over a 24 hour period to improve the ion exchange process. The PSF-TMA$^+$ in the sulfate form was immersed and rinsed with DI water for several hours (at least 3 hours) to remove excess ions.

Ionic conductivity. Electrochemical impedance spectroscopy (EIS) was used to determine the in-plane conductivity of the membrane. A membrane (in sulfate form) was placed in the conductivity cell (Teflon® cell) in contact with 4 platinum wires. The external wires were connected to the working and counter electrodes of the potentiostat and the inner electrodes were used as working sense and reference.

The conductivity cell was immersed in DI water and kept in a thermostatic bath. A Gamry potentiostat (Series G750) was used to measure the in-plane membrane impedance in the frequency range 100,000 to 0.1 Hz. High frequency resistance along with membrane thickness and width were used to estimate membrane ionic conductivity. The ionic conductivity value of the membrane was determined using the following equation:

$$\sigma = \frac{L}{R \times t \times w} \quad (1)$$

Where, σ is in-plane conductivity, R is in-plane membrane resistance, t is membrane thickness (of the fully hydrated membrane), and w is membrane width (of the fully hydrated membrane).

Permeability. Vanadium (IV) permeability (VO^{2+}) was measured by monitoring the amount of VO^{2+} moving across the membrane as a function of time. The membrane was placed in-between two compartments of a diffusion cell (20 mL diffusion cell from PermeGear Inc. with an effective area of 4.91cm^2). One compartment was filled with 10 mL of 1.5 M $VOSO_4$ [V (IV) – VO^{2+}] in 3 M H_2SO_4 solution and the other compartment was filled with 20 mL of 1.5 M Na_2SO_4 in 3 M H_2SO_4 solution. Samples from the diluted side (Na_2SO_4 solution) were withdrawn at predetermined time intervals. The absorbance was measured at a wavelength of 745 nm and used to calculate (with a previously build calibration curve) the concentration of VO^{2+}. Membrane permeability was calculated using following equation:

$$P = \frac{V_B \times d}{C_A \times A} \times \frac{dC_B}{dt} \quad (2)$$

where P is the membrane permeability, V_B is the volume of solution in diluted side (20 mL), d is the thickness of the membrane, C_A is the concentration of VO_2SO_4 in the concentrated side (1.5M), A is the effective area of membrane contacting to the solution (4.91 cm^2) and dC_B/dt is the change of the concentration with time (measured from experimental data). Multiple experiments were done to assure reproducibility.

Ex-situ oxidative stability test. The *ex-situ* oxidative stability of membrane was evaluated by monitoring ionic conductivity and chemical structure (via NMR spectra) before, during, and after immersion in electrolyte solution with 1.5 M VO_2^+ in 3 M H_2SO_4. Membrane samples and electrolyte solution were placed in vials and the vials were placed in an oven at 30 ^oC.

NMR characterization. All NMR measurements were carried out on a Bruker Avance 360 MHz NMR spectrometer. The NMR experiments performed were as follows: 1D ^1H (spectra collected at 360 MHz), ^{13}C (spectra collected at 90 MHz – proton decoupled), and 2D ^1H-^1H correlation spectroscopy **(**COSY), and ^1H-^{13}C heteronuclear multiple-quantum correlation spectroscopy (HMQC). Table S1 provides the information for 2D NMR experiments. Sample preparation for NMR spectra acquisition was as follows: 30 to 40 mg of sample was dissolved into 1 mL of deuterated solvent - dimethylsulfoxide (DMSO-d6). Tetramethylsilane (TMS) was added as an internal standard for all samples. Note: CMPSF (PSF-TMA^+ precursor) spectra are not reported in this work. Our previous work documents NMR spectra for this sample.[3] The determination of quaternary ammonium groups was done by integrating the ^1H NMR spectra (see equation 3).

$$\text{Remaining percentage of cation sites} = \frac{\text{Area}_{\text{cation substituent}}\ (\delta \approx 3.0\text{ to }3.1\text{ ppm})}{\text{Ratio} \times \text{DF} \times \text{Area}_{\text{PSF substituent}}\ (\delta \approx 1.7\text{ ppm})} \qquad (3)$$

Ratio is the number of protons in the cation substituent (n=9; label 7 in Fig. S1) divided by the number of protons found in the iso-propyl substituent in the backbone (n=6; label 8 in Fig S1). *Ratio* = 1.5

DF is the degree of chloromethylation functionalization to the PSF backbone. For this study, the *DF* value was 0.9.

Area is the integrated peaks in the ^1H NMR spectra

δ is the chemical shift of the peaks in the ^1H NMR spectra

Table S1. Details and parameters for 2D NMR experiments

Technique	Details
COSY	2D homonuclear shift correlation using gradient pulses for selection Incremental resolution: 1024 x 128 Number of scans: 4
^1H-^{13}C HMQC	2D HMQC ^1H-1/X correlation via heteronuclear zero and double quantum coherence with decoupling during acquisition. Used gradient pulses for selection Incremental resolution: 1024 x 128 Number of scans: 10

Water uptake, swelling, elongation, and stress-strain behavior of the ion exchange membranes. Water uptake in the vapor phase as a function of relative humidity was measured with a vapor sorption analyzer (TA instruments VTI SA+) at 25 °C. Vacuum dried samples were loaded into the VTI-SA+ to start the experiment. The membranes were allowed to equilibrate for 180 minutes at each relative humidity before recording the water uptake. The water uptakes for samples immersed in DI water (18 MΩ) were determined using procedure given in our previously published work.[2] The procedure is summarized as follows: vacuum dried samples were weighed and then immersed in DI H_2O and stored in oven set to 30 °C. After 24 hours, the surface of the samples were swabbed and patted dry to remove excess liquid from the surface and the weights of the samples were recorded. Equation 4 was used for determining the water uptake and equation 5 was used for determining the lambda value. The creep compliance test (i.e., strain as a function of relative humidity at 25 °C) for the ion-exchange membranes was performed on a TA instruments Q800 dynamic mechanical analyzer using a humidity chamber. The membrane sample (approximate dimensions: 50 mm x 5 mm x 0.05 mm) was fixed in a film tension clamp using a torque of 3 lbF x in. The set force during the measurement was 0.1 N and the temperature was 25 °C. The humidity was ramped 0 to 98% relative humidity (RH) at 2% RH per minute. The stress-strain curves of the ion-exchange membranes were determined with a Q800 differential mechanical analyzer (TA instruments) using a humidity chamber. The membrane sample (approximate dimensions: 50 mm x 5 mm x 0.05 mm) was fixed in a film tension clamp using a torque of 3 lbF x in, and heated to 50 ^oC under 50 % RH. The membrane was allowed to equilibrate for 60 minutes before starting the test. The membrane was stretched at 0.5 MPa min^{-1} until the sample broke.

$$\mathrm{WU} = \frac{\mathrm{Wt}_{\mathrm{hydrated}} - \mathrm{Wt}_{\mathrm{dry}}}{\mathrm{Wt}_{\mathrm{dry}}} \,\mathrm{x}\, 100\% \qquad (4)$$

$\mathrm{Wt}_{\mathrm{hydrated}}$ = Weight of the membrane fully hydrated

$\mathrm{Wt}_{\mathrm{dry}}$= Weight of the membrane dried

$$\lambda = \frac{\mathrm{WU}\cdot 1000\frac{\mathrm{mmol}}{\mathrm{mol}}}{(\mathrm{IEC}\cdot 18.015\frac{\mathrm{g}}{\mathrm{mol}}\cdot 100\%)} \qquad (5)$$

WU = WU = Water uptake of the sample (%)

Redox flow battery testing. Redox flow battery (single cell) testing was carried out in an acid-resistant fuel cell hardware (Fuel Cell Technologies, Inc). The MEA (5 cm^2 active area) was assembled by sandwiching a membrane between two carbon felt electrodes (3.18 mm thick, Alfa Aesar). The negative and positive electrolytes were 1.5 M V^{2+}/V^{3+} and 1.5 M VO^{2+}/VO_2^{+}, respectively, both in 3 M H_2SO_4 solution. The electrolytes were prepared by electrolysis of 1.5 M VO_2SO_4 + 3 M H_2SO_4 solution. Anolyte and catholyte were recirculated (1 mL min^{-1} for the experiments at 30 mA cm^{-2} and 50 mL min^{-1} for the experiments at 100 mA cm^{-2}) through the graphite flow fields using two peristaltic pumps (Gilson Minipuls). The volume of anolyte and catholyte solutions was 5 mL (in each side). Charge/discharge testing was conducted at constant current density (30 mA cm^{-2} or 100 mA cm^{-2}) at room temperature. The cutoff voltages for charge and discharge were 1.7 and 0.65 V; charge or discharge cycles were deemed finished when the current density dropped below (4 mA cm^{-2}). The Coulombic efficiency (CE) is defined as the discharge capacity (A-h) divided by the charge capacity. Energy efficiency (EE) is defined as the discharge energy (W-h) divided by the charge energy, and the voltage efficiency (VE) was calculated as VE = EE/CE.

SEM imaging and XEDS. Prior to scanning electron microscopy (SEM) analysis, the samples were rinsed excessively with deionized water and then air dried overnight. A Hitachi S-3000N (Hitachi, Ltd. Japan) with a variable pressure chamber was used to image the AEM samples. The pressure of the sample chamber was 100 Pa and the accelerating voltage was 20.0 kV. The resolution of the images reported are x800. The XEDS spectra were collected with the same instrument containing an Oxford Inca XEDS system with a light element x-ray detector (15 mm working distance).

Results from permeability experiments

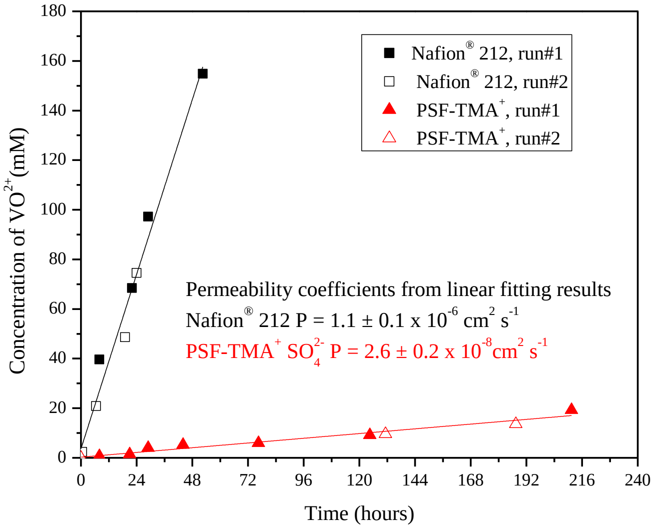

Figure S1. VO^{2+} concentration accumulation in the dilute side of the concentration cell versus time using a PSF-TMA$^+$ AEM or Nafion® 212 separator. The data presented illustrates the large difference in vanadium (IV) (VO^{2+}) permeability between the two membranes.

2D NMR COSY PSF-TMA$^+$ results after exposure to 1.5 M VO_2^+ for 90 days

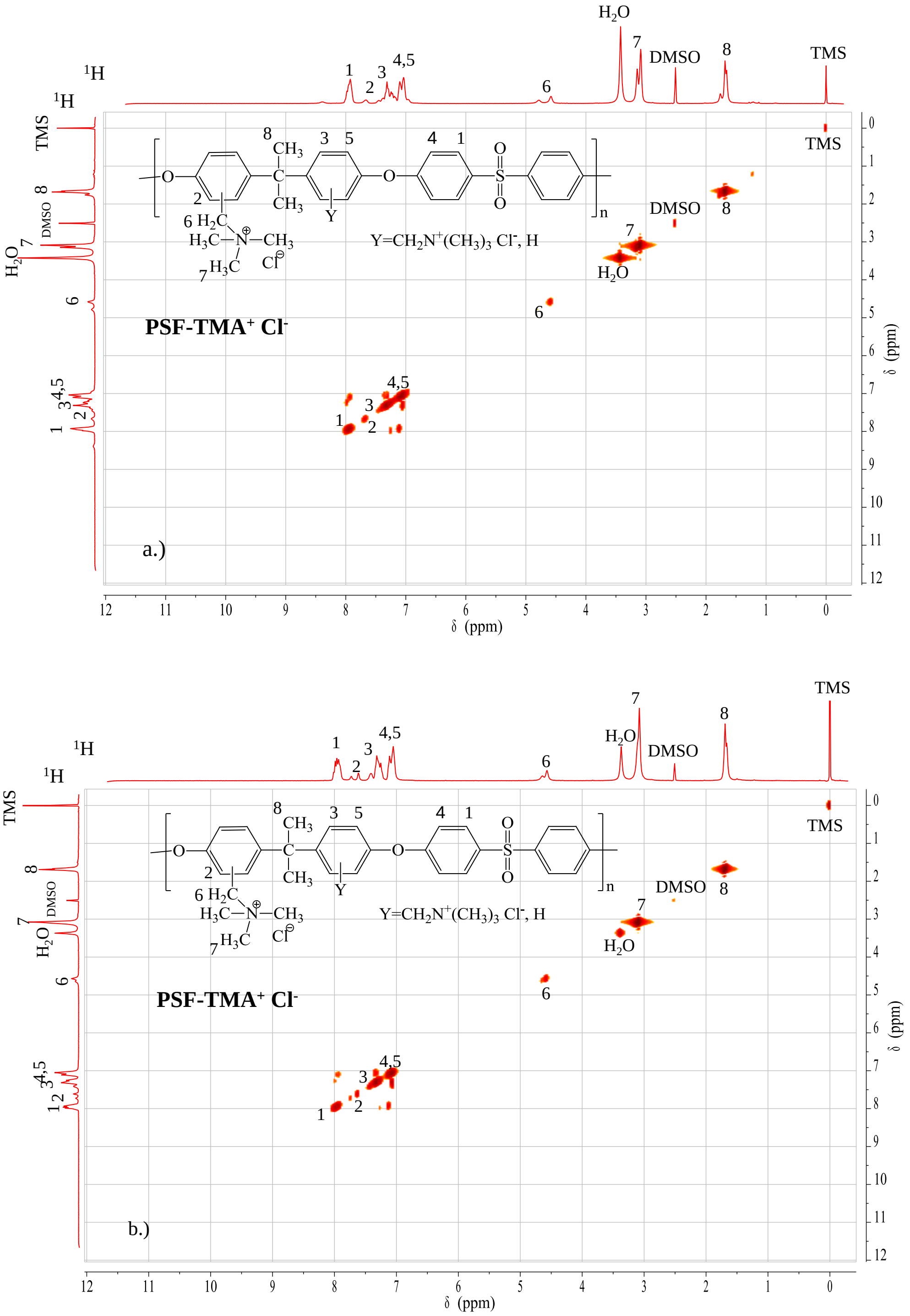

Figure S2. COSY NMR spectra of PSF-TMA$^+$ (a) before and (b) after exposure to 1.5M VO_2^+ [V(V)] in 3 M H_2SO_4 at 30°C for 90 days.

2D NMR of PSF-TMA$^+$ post-mortem analysis after charge-discharge in a VRFB during 140 h.

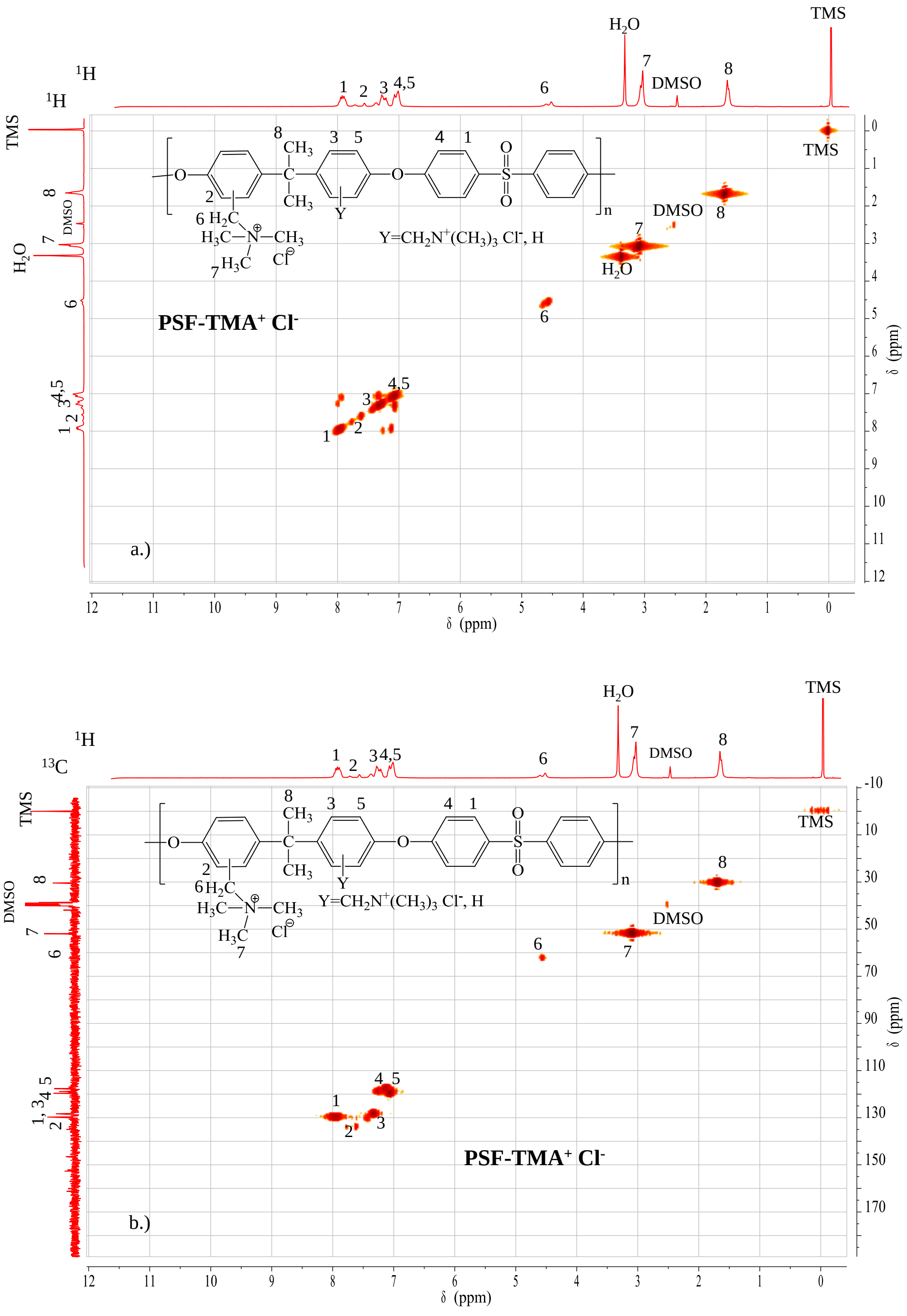

Figure S3. Post-mortem 2D NMR spectra of PSF-TMA$^+$ after VRFB charge/discharge cycling during 140 h; (a) COSY spectrum and (b) ^{1}H-^{13}C HMQC spectrum. This membrane came from the battery cycling test at 30 mA cm^{-2} for 35 cycles.

Additional VRFB results

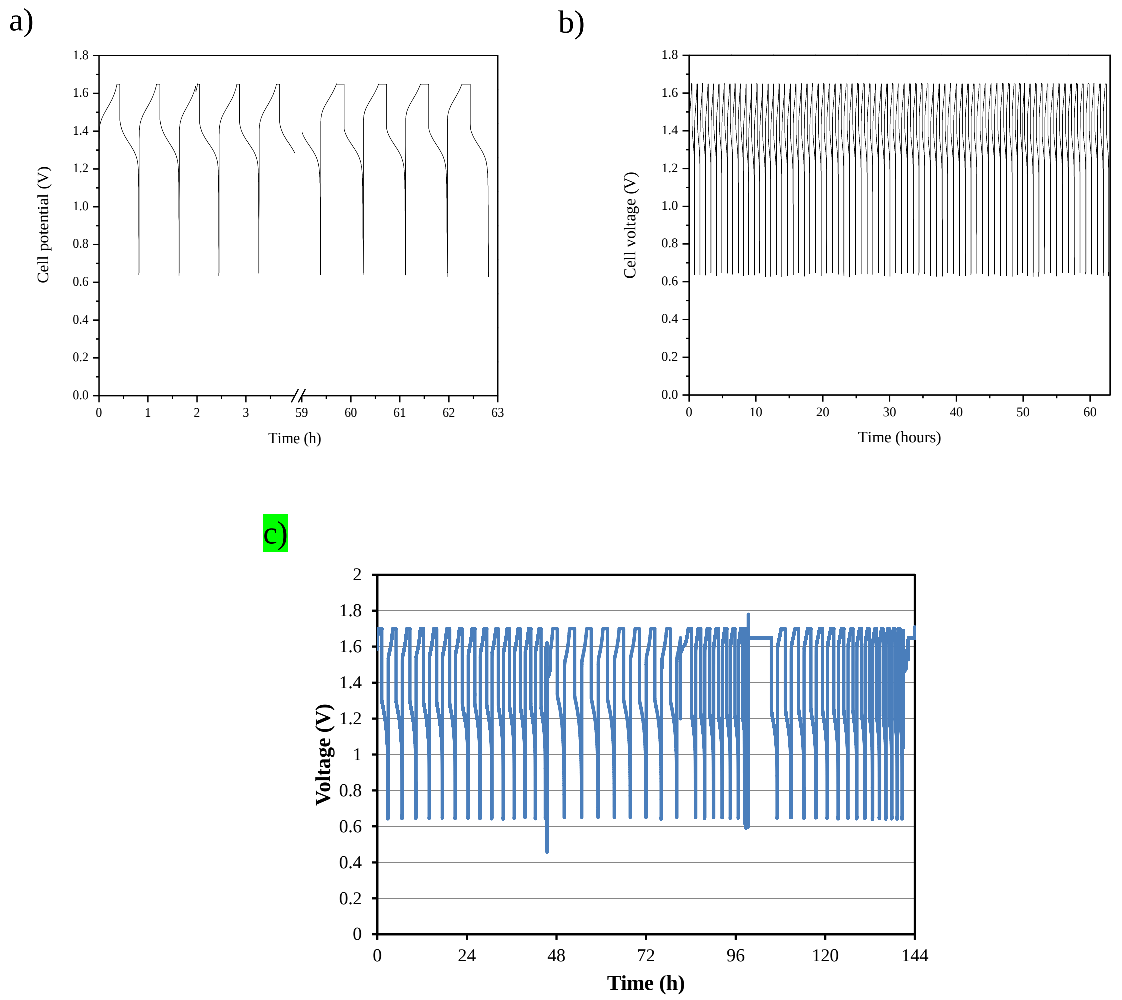

Figure S4. Voltage profiles of cycling a VRFB using a PSF-TMA$^+$ SO$_4^{2-}$ separator at different current densities. a.) Focused voltage profiles (for clarity) during charge/discharge cycling at 100 mA cm^{-2}. The left-side of the graph depicts the voltage profile while cycling the battery during the first four hours and the right hand side of the graph depicts the voltage profile during the final four hours. b.) Voltage profiles during all 75 charge/discharge (60 hours of operation) cycling at 100 mA cm^{-2}. c.) Voltage profiles during all 35 charge/discharge (144 hours of operation) cycling at 30 mA cm^{-2}.

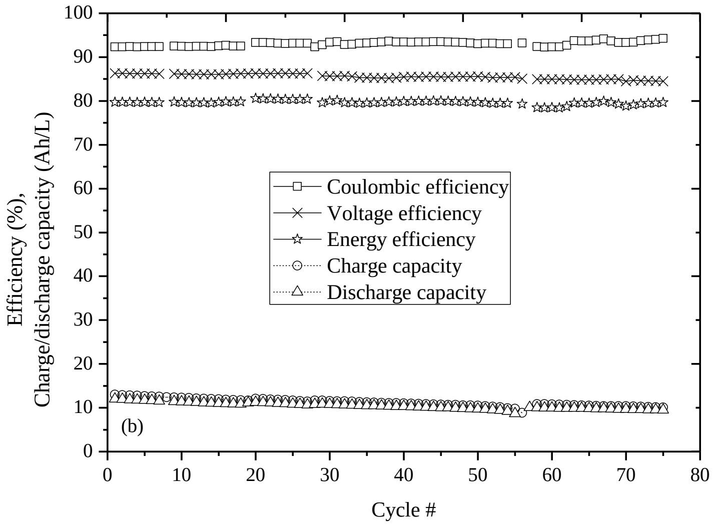

Figure S5. Effect of charge-discharge cycling on the coulombic, energy and voltage efficiencies and battery charge-discharge capacities for Nafion® 212. The current density was 100 mA cm^{-2}.

Water uptake, swelling, and elongation results

Water uptake, swelling, and elongation of polysulfone-based AEMs and Nafion®. Figure S6 provides the water uptake data and lambda values (number of water molecules per ion-exchange site – intrinsic water uptake for a material) as a function of relative humidity for PSF-TMA$^+$ SO_4^{2-} (polysulfone with quaternary benzyl trimethylammonium sulfate) and Nafion® 212. The water uptake was measured in a well-controlled water sorption analyzer (which can only operate in the vapor phase), which allowed for accurate water uptake measurements. Although this experiment does not directly mimic the conditions in the VRFB, it was decided that the measurements using the vapor sorption analyzer would be accurate and of value. The water uptake and swelling ratio measurements performed by immersing the membrane in a liquid solution and measuring the weight gain (or film expansion) has issues related to accuracy and precision. After the samples have equilibrated in immersed solution, they need to be quickly removed from the solution and swabbed to remove excess water from the surface. The water removal step can vary from operator to operator and is not an optimal means to determine the water uptake or swelling ratio value. Furthermore, the transition of taking the swabbed sample and moving it to a balance to make a weight measurement allows for a transient period where water can evaporate from the sample. Both of these processes can lead to inaccurate and imprecise water uptake data. Despite these possible experimental flaws, the water uptake and swelling ratio of the membranes immersed in liquid deionized (DI) water were also determined. The water uptake in DI water for PSF-TMA$^+$ SO_4^{2-} was 37 ± 1% and for Nafion® 212 it was 15 ± 1%. The lambda value for PSF-TMA$^+$ SO_4^{2-} was 13.5 and for Nafion® 212 it was 9.2. The swelling ratio (the expansion of the length dimension (long side)) in DI water for PSF-TMA$^+$ SO_4^{2-} was 9 ± 1% and for Nafion® 212 it was 5± 1%. The lambda values for the PSF-TMA$^+$ SO_4^{2-} were slightly higher than Nafion® 212 since the polytetrafluoroethylene (PTFE) backbone in Nafion® is more hydrophobic than the hydrocarbon backbone present in the polysulfone.

Figure S7 reports the creep compliance versus relative humidity (i.e., strain/elongation – expressed as a percentage) of PSF-TMA$^+$ SO_4^{2-} and Nafion® 212 under a constant force (0.1 N). As the humidity increased, the strain of the Nafion® 212 grew larger when compared to PSF-TMA$^+$ SO_4^{2-}. The creep compliance response to relative humidity for Nafion® 212 was larger than PSF-TMA$^+$ SO_4^{2-} since the modulus of PSF-TMA$^+$ SO_4^{2-} was larger than Nafion®. See Figure S8 for the stress-strain curve comparison of Nafion® versus PSF-TMA$^+$.

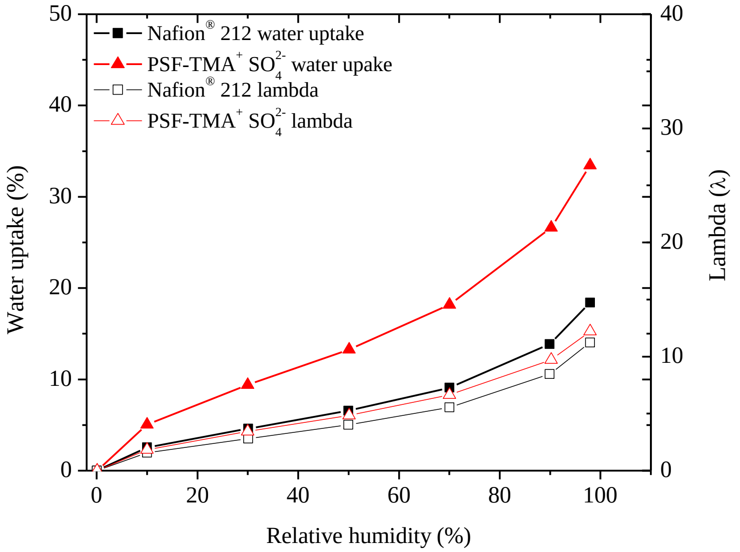

Figure S6. Water uptake and lambda as a function of relative humidity at 25 ^{o}C for PSF-TMA^{+} SO$_4^{2-}$ and Nafion® 212.

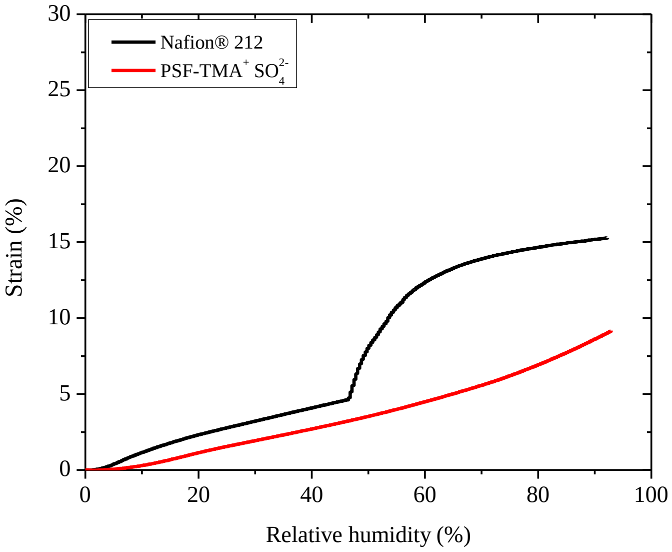

Figure S7. Comparison of strain versus relative humidity at 25^{o}C for PSF-TMA^{+} SO$_4^{2-}$ and Nafion® 212.

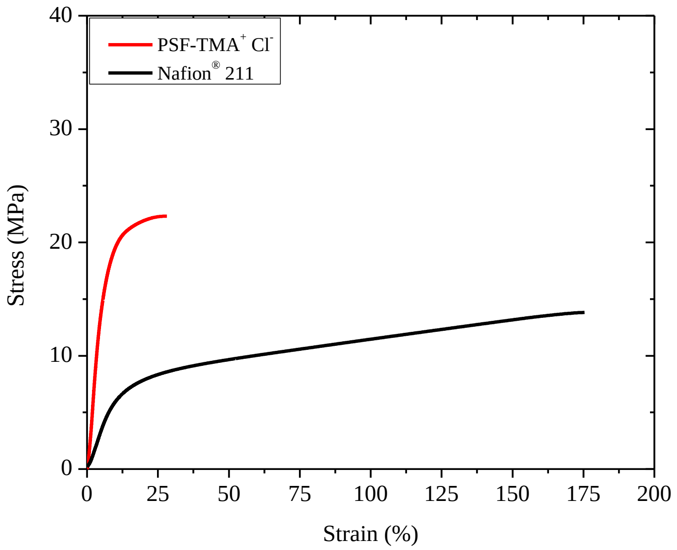

Figure S8. Stress-strain curve of PSF-TMA$^+$ and Nafion®. The modulus was larger in the linear viscoelastic region for PSF-TMA$^+$ when compared to Nafion®.

XEDS results

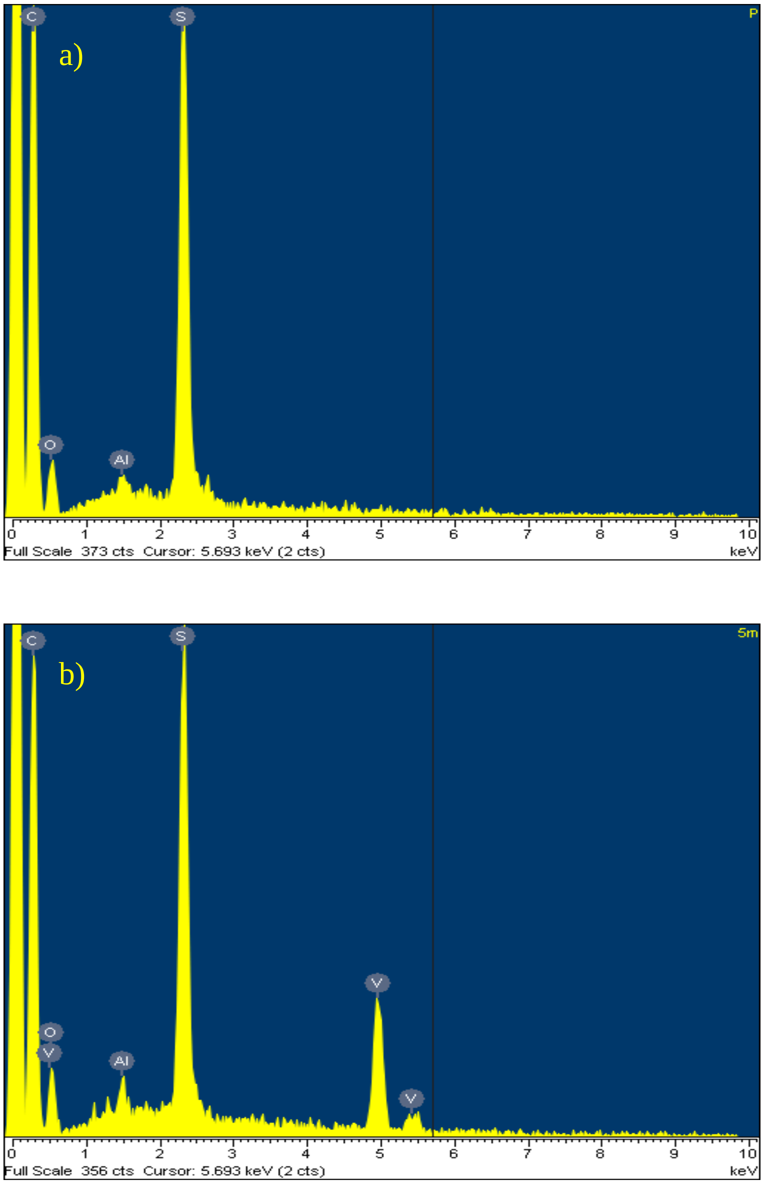

Figure S9. X-ray energy dispersive spectra (XEDS) of PSF-TMA$^+$ (a) before and (b) after exposure to 1.5M VO_2^+ in 3 M H_2SO_4 at 30 °C for 90 days. The spectrum in b) shows the presence of vanadium species imbedded on the surface of the membrane after exposure to 1.5M VO_2^+ in 3 M H_2SO_4 at 30 °C for 90 days. Polysulfone AEMs contain the other elements of carbon, sulfur and oxygen (the peaks appear clearly in both spectra). The detected aluminum comes from the sample holder.

References

1. E. Avram, E. Butuc, C. Luca and I. Druta, *J. Macromol. Sci., Pure Appl. Chem.*, 1997, **A34**, 1701-1714.
2. C. G. Arges, J. Parrondo, G. Johnson, A. Nadhan and V. Ramani, *Journal of Materials Chemistry*, 2012, **22**, 3733-3744.
3. C. Arges and V. Ramani, *Proc. Natl. Acad. Sci. U. S. A.*, 2013, **110**, 2490-2495.